Numerical calculation of separated flow past square and rectangular cylinders using panel technique

A. Roy
Department of Space Engineering and Rocketry
Birla Institute of Technology,
Mesra, Ranchi, India

G. Bandyopadhyay
Department of Aerospace Engineering
Indian Institute of Technology
Kharagpur, India

ABSTRACT

In the present investigation, a potential flow model based on panel method has been developed for calculation of two dimensional separated flows past square and rectangular cylinders. Free vortex lines are assumed to emanate from the points of separation that converge downstream of the body. The converged wake shape is iteratively obtained by integrating the velocity vectors at the collocation points. For solving separated flow past square and rectangular cylinders, four different versions of the solver have been developed for a wide range of incidence, namely, for zero, low, moderate and high angles of incidence. For validation of computed results, experimental investigations have been carried out in a low speed wind tunnel to obtain the surface pressure distribution on square cylinder and rectangular cylinder over a range of angles of incidence. Comparison is reasonably good.

NOMENCLATURE

A_{ji}, A'_{ji}, B_{ji}, B'_{ji}	influence coefficients due to linearly varying vorticity and constant source distribution on the cylinder
C_{ji}, C'_{ji}, D_{ji}, D'_{ji}	influence coefficients due to vorticity distribution on upper and lower wake
AR	aspect ratio of rectangular cylinder (= L/B)
B	length of side of square cylinder and height of rectangular cylinder
C_D	drag coefficient
C_L	lift coefficient
C_P	pressure coefficient
ΔH	decrease in total pressure in the wake over that in the free stream
L	length of rectangular cylinder
NW	number of panels on upper and lower shear layers
N	number of body surface panels
p_∞	free stream static pressure
q	magnitude of total velocity
Re	Reynolds number
s	distance along shear layer
S	running co-ordinates on cylinder surface
S_u, S_l	total length of upper and lower shear layer
u, v	normalised perturbation velocities
U_∞	free stream speed
x, y	Cartesian co-ordinate system

Subscripts

av	average
c	wake closure
ji	panel indices, i is field point and j is collocation point
inner	point just adjacent to a shear layer and inside the wake

Paper No. 2946. Manuscript received 17 December 2005, revised version received 22 December 2005, accepted 23 January 2006.

https://doi.org/10.1017/S0001924000001226 Published online by Cambridge University Press

l, lower	lower shear layer
outer	point just adjacent to a shear layer and outside the wake
u, upper	upper shear layer
wake	point inside the wake
∞	free stream
1	first upper or lower shear layer panel

Greek symbols

α	angle-of-incidence
γ	vorticity strength
σ	source strength
λ	vorticity dispersion factor
ρ	density

1.0 INTRODUCTION

The problem of separated flow past bluff bodies of various geometries like circular, triangular, square and rectangular cylinders has attracted widespread attention of large number of researchers around the world during the last few decades. This problem is of immense importance in diverse fields of engineering due to its widespread application in different configurations.

To get an insight to the aerodynamic characteristics of separated flow past square and rectangular bodies, numerous experimental studies have been conducted over the past few decades to obtain the aerodynamic characteristics of bluff bodies. Experimental measurements of the mean and fluctuating pressure field acting on a two-dimensional square cylinder in uniform and turbulent flows have been presented by Lee[1] at Re = $1{\cdot}76 \times 10^5$. Experimental mean and fluctuating pressure on a two-dimensional square cylinder in uniform flow at Re = $1{\cdot}4 \times 10^5$ has been reported by Robertson *et al*[2]. The authors investigated the nature of the separation-reattachment phenomenon occurring on the side wall of the cylinder for angles of incidence varying from –50° to 90°. Igarashi[3] has carried out experimental investigations on the characteristics of the flow around a square cylinder at angles of incidence varying from 0° to 45° in the range of Reynolds number varying from Re = $1{\cdot}1 \times 10^4$ to $5{\cdot}6 \times 10^4$. Mean and fluctuating pressure on the surface of the cylinder as well as Strouhal number, lift and drag coefficient as function of Reynolds number and angle of incidence have been obtained. Flow visualisation using smoke and oil flow have revealed the reattachment point on the side face of the cylinder as a function of angle of incidence. Chen and Liu[4] have experimentally investigated the vortex shedding frequencies and surface pressure of a square cylinder at non-zero angles of incidence over a Reynolds number range of Re = 2,000-21,000.

Detailed experimental investigation of flow past rectangular cylinders of aspect ratios varying from 0·5 to 4·0 are reported in Igarashi[5] and aspect ratio 6·0 is reported in Sam *et al*[6]. Experiments on flow characteristics around two-dimensional rectangular cylinders in the range of Reynolds numbers $2{\cdot}56 \times 10^4 - 5{\cdot}77 \times 10^4$ have been studied at $\alpha = 0°$ by Igarashi[5]. Bearman and Trueman[7] found that aerodynamic characteristics of rectangular cylinder of aspect ratio 0·67 are drastically different as compared to rectangular cylinders of other aspect ratios. The paper of Da Matha Sant Anna *et al*[8] deals with smooth flow around rectangular cylinders of aspect ratio varying from 0·5 to 3·0 at Reynolds number 10^5. Measurements of mean surface pressure distribution at different angles of incidence have been reported. A comprehensive analysis of the phenomena associated with shear layer reattachment and the separation bubble formation for varying aspect ratios and angles of incidence has been attempted. At zero angle of incidence the observations are very similar to those of Igarashi[5]. Laneville and Yong[9] studied the flow field past rectangular cylinders of various aspect ratio at zero angle of incidence and attempted to develop some empirical correlations to characterise the flow pattern. Some other experimental investigations on square and rectangular cylinders are reported by Obasaju[10], Nakaguchi *et al*[11] and Bostok and Mair[12].

These experiments reveal some of the features of the flow past square and rectangular cylinders. Sharp edges of such bodies do fix separation and unlike for smooth bodies e.g. circular cylinder, the separation points do not change with Reynolds number or surface roughness. However, the separation points change with angle of incidence and the flow pattern for different angles of incidence can be categorised into four regimes, as shown in Table 1.

The problem in calculating such separated flows is that the governing equation of the real viscous flow is the Navier-Stokes equation which is not easily amenable to solution, particularly for high Reynolds number. This has prompted many researchers to develop 'inviscid flow models' which combine a panel (singularity) technique with appropriate vortex shedding model. However, the characteristics of the viscous wake including dissipation and diffusion and also cancellation of the vorticity in the neighbourhood of the wake closure are difficult to understand and hence difficult to simulate properly in such inviscid flow models.

The variety of inviscid flow models developed so far can be broadly classified into two categories. In the first category of methods, the free shear layers, which emanate from the body are represented by an assembly of discrete vortices. These 'discrete vortex methods' (DVM) have been elaborately discussed by Sarpkaya[13]. In such methods, the strengths and positions of nascent vortices are determined by criteria of rate of shedding vorticity and by the Kutta condition. Inamuro *et al*[14] developed a discrete vortex method and obtained result for a square cylinder for angle-of-attack of 0°, 10°, 20° and 30°. In this method Kutta condition was not satisfied and vortices were assumed to be shed from the two front corners only. Consequently, the model failed to take the effect of reattachment on the lower surface around $\alpha = 14°$ and also flow around $\alpha = 45°$ i.e. reattachment or wedge flow could not be calculated. Sarpkaya and Ihrig[15] investigated both experimentally and numerically the impulsively started flow about square and rectangular prisms. Results presented for $\alpha = 1°$, 5° and 10° show reasonably good agreement between predicted and measured forces with respect to frequency of the oscillations, i.e., Strouhal number. However, amplitudes of the predicted forces were somewhat larger. More realistic results were achieved by considering vortex decay in the wake due to viscous dissipation and diffusion by vortex blob, random walk, circulation reduction techniques for numerous bluff body flows. Notable examples are the works of Nagano *et al*[16] and

Table 1
Categorisation of flow past square bodies

Angle of incidence	Flow characteristics	Separation points
$\alpha = 0°$	symmetric flow	front top and bottom corner
$1° \le \alpha \le 13°$	asymmetric flow	front top and bottom corner
$14°\sim15° \le \alpha \le 35°$	reattachment flow	front top and bottom corner (with reattachment on bottom surface followed by separation from rear bottom corner)
$36° \le \alpha \le 45°$	wedge flow	front top and rear bottom corner

https://doi.org/10.1017/S0001924000001226 Published online by Cambridge University Press

Stansby[17] for rectangular prism, Sarpkaya and Schoaff[18] for circular cylinder, Basuki and Graham[19] for aerofoil, etc.

In the second category of methods, the separation in the wake is simulated by using vortex lines instead of discrete vortices. The literature on the 'line vortex method' (LVM) is less developed in comparison to discrete vortex methods. The pioneering work in developing such line vortex method is due to Maskew and Dvorak[20]. They developed an iterative procedure between potential flow and boundary layer solution for analysis of airfoils up to and beyond stall. The separated region is modelled in the potential flow analysis using 'free vortex lines' which require an inner iteration to establish their shapes.

A more physically realistic model based on constant vortex singularity on the body and 'free vortex lines' on the wake has been developed by Ribaut[21] in which viscous dispersion of vorticity in the wake is taken into consideration. Vorticity dispersion is taken into account by assuming a linear reduction in vorticity strength in the downstream direction on the free vortex lines. He demonstrated that the extension and underpressure of the wake of a flat plate with blunt trailing edge section are essentially determined by the amount of viscous diffusion and dissipation of the vorticity in the wake.

Another line vortex model based on panel method, employing linearly varying vorticity distribution on the body, was developed by Mukherjea and Bandyopadhyay[22] for calculating separated flow about a non lifting wedge configuration. If vorticity is assumed to be constant in the wake, the model gives an infinite extension of the wake and constant base pressure. However, incorporation of dispersion of vorticity in the wake leads to its finiteness and non-uniform underpressure. Numerical results agree closely with experimental values for different wedge configurations for specific values of dispersion factors.

In the present investigation, an inviscid flow model based on panel technique has been developed for calculation of bubble-type separated flow problem. The model uses linearly varying vorticity and constant source singularity on the body and piecewise constant line vortex panels on the wake. To take the effect of vorticity dispersion in the wake the vorticity strength is assumed to decay linearly along the free vortex lines in the wake.

The model has been applied to flow past square and rectangular cylinders for all flow regimes mentioned in Table 1, i.e. symmetric, asymmetric, reattachment and wedge flows covering $\alpha = 0°$-$45°$. To accomplish this, four different versions of the model, with appropriate separation points, have been developed for the four flow regimes. Special care has been taken for the reattachment flow regime by modifying the bottom surface of the body to include the closed bubble and singularities are placed on the 'modified body surface'.

Availability of computed or experimental pressure distribution on the body surface for the entire range of angle of incidence from 0° to 45° is not so common. In order to compare the numerical accuracy of the present model experiments have been conducted on square and rectangular cylinders in a low speed wind tunnel. The experimental work involves measurement of pressure on a square cylinder and a rectangular cylinder of aspect ratio 2 using pressure transducer/scanivalve assembly. Experimental results were obtained at Reynolds number $1{\cdot}96 \times 10^5$.

2.0 DISCRETISED MODEL FOR SQUARE AND RECTANGULAR CYLINDERS

The surface of the square and rectangular cylinders is divided into a large number of panels N (usually 120) on each of which source and vorticity singularities are distributed. The strength of the vorticity distribution is assumed to be linearly varying across each panel on the body surface. The value of the vorticity at the start of the i-th panel is denoted by γ_i and at the end by γ_{i+1}. However, the strength of the source distribution σ is assumed to be constant for each panel. The wake is enclosed by two shear layers emerging from the separation points. Each shear layer is divided into NW (usually 80) number of panels on which vorticity singularities are placed. With no dispersion of vorticity in the wake, vorticity strength remains constant along the entire wake length. If dispersion of vorticity in the wake is taken into consideration, vorticity strength remains constant for a particular panel but decreases linearly downstream along the wake after the first wake panel.

Figure 1(a) shows the discretisation of the square cylinder surface and the shear layers which model the wake at zero angle of incidence ($\alpha = 0°$). Figure 1(b) shows the discretised model at low angles of incidence ($1° \le \alpha \le 13°$) where the flow separation points remain unaltered, but the wake becomes asymmetrical. The discretised model at moderate angles of incidence ($14°$~$15° \le \alpha \le 35°$) is shown in Fig. 1(c). This flow field is associated with the formation of a separation bubble at the bottom face of the body and the separation points are located at the top corner of the front face and the bottom corner of the rear face. A 'modified body approach' has been formulated in the present investigation to model the separation bubble. Body surface panels have been distributed on the separation bubble surface and the pressure distribution on the bubble has been assumed to be equal to the pressure acting on the body surface below the bubble. Figure 1(d) shows the discretised model used to solve separated flow at high angles of incidence ($36° \le \alpha \le 45°$) in which the separation points are at the top corner of the front face and bottom corner of the rear face, but there is no separation bubble formation on the bottom face.

The solution for the unknown singularity strengths is obtained by satisfying the boundary condition of zero normal flow at the collocation points of the panels on the cylinder surface together with the appropriate Kutta condition at the separation points. There are (N+1) unknown nodal vorticity strengths (λ_1 to λ_{N+1}), and an unknown source strength (σ), making a total of (N+2) unknowns. The vorticity strengths of the wake panels do not constitute any additional unknowns as they are expressed in terms of the vorticity strengths of body surface panels at separation points.

Satisfaction of the boundary condition of zero normal velocity at the N collocation points on the surface panels gives rise to N equations. Two other equations are obtained by applying two auxiliary conditions at the separation points and trailing edge, making a total of (N+2) equations for (N+2) unknown singularity strengths.

Let $\bar{u}$ and $\bar{v}$ be the normalised perturbation velocities due to the singularity distribution on the cylinder and the wake. These velocity components can be expressed as

$$\bar{u}_j = \sum_{i=1}^{N+1} A_{ji} \times \bar{\gamma}_i + \bar{\sigma} \times \sum_{i=1}^{N} B_{ji} + \sum_{i=1}^{NW} C_{ji} \times \bar{\gamma}_{ui} + \sum_{i=1}^{NW} D_{ji} \times \bar{\gamma}_{li} \quad \ldots (1)$$

$$\bar{v}_j = \sum_{i=1}^{N+1} A'_{ji} \times \bar{\gamma}_i + \bar{\sigma} \times \sum_{i=1}^{N} B'_{ji} + \sum_{i=1}^{NW} C'_{ji} \times \bar{\gamma}_{ui} + \sum_{i=1}^{NW} D'_{ji} \times \bar{\gamma}_{li} \quad \ldots (2)$$

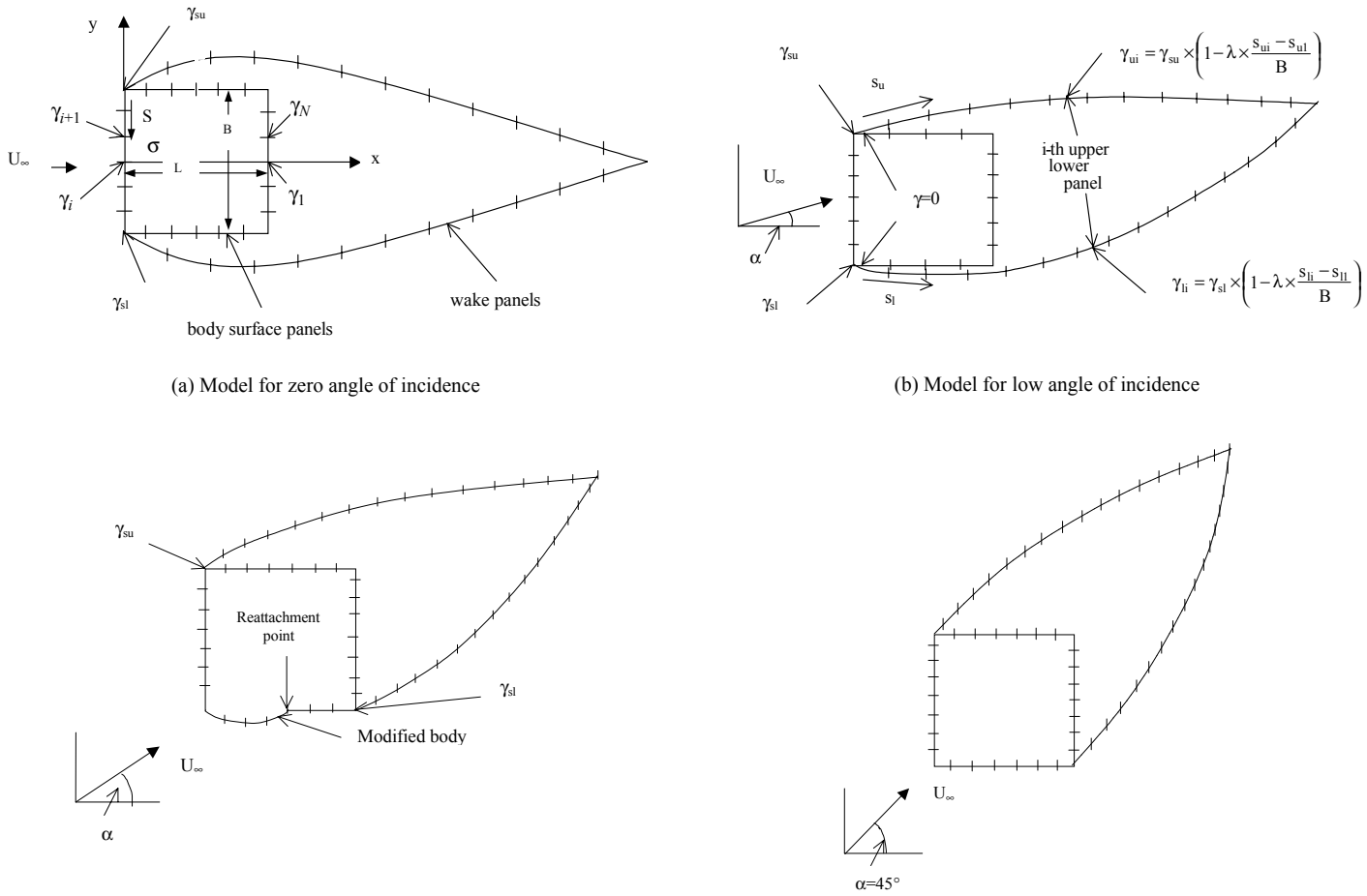
where A_{ji} and A'_{ji} are the influence coefficients of the nodal values of linearly varying vorticity distribution on the cylinder, B_{ji} and B'_{ji} are the influence coefficients of the constant source distribution on the cylinder, C_{ji} and C'_{ji} are the influence coefficients of the upper wake, and D_{ji} and D'_{ji} are the influence coefficients of the lower wake at the j-th panel collocation point.

$\bar{\gamma}_{ui}$ and $\bar{\gamma}_{li}$ are the vorticity strengths at the midpoints of the i-th upper and lower wake panels respectively. If no dispersion of vorticity in the wake is assumed then vorticity strength on all upper and lower wake panels remain same downstream, and are equal to nodal vorticity strengths at the separation points, i.e.,

$$\bar{\gamma}_{ui} = \bar{\gamma}_{su}$$
$$\bar{\gamma}_{li} = \bar{\gamma}_{sl} \quad \ldots (3)$$

However, assumption of constant vortex strength in the wake leads

https://doi.org/10.1017/S0001924000001226 Published online by Cambridge University Press



(a) Model for zero angle of incidence

(b) Model for low angle of incidence

(c) Model for moderate angle of incidence

(d) Model for high angle of incidence

Figure 1. Discretised models for square cylinder.

to constant underpressure in the wake and an infinite extension of the wake. Also, it is likely to be too restrictive in the case of a real fluid flow. In real fluid flow, pressure rise occurs through the process of turbulent mixing in the fluid in and near the shear layer and between the two shear layers in the neighbourhood of closure. Consequently, the vorticity in the wake in a real fluid flow can be characterised by the dispersion of vorticity in the wake through dissipation and diffusion and also cancellation of vorticity in the neighbourhood of closure.

To account for the subsequent dispersion of vorticity in the wake, a piecewise constant vorticity model for the wake is considered in which the vorticity strength in the wake is assumed to be decreasing downstream after first separation panel. However, vorticity strength in each wake panel is assumed to be constant. These vorticity strengths can be expressed as functions of the nodal vorticity strengths at the separation points ($\bar{\gamma}_{su}$ and $\bar{\gamma}_{sl}$) respectively as

$$\bar{\gamma}_{ui} = \bar{\gamma}_{su} \times \left(1 - \lambda \times \frac{s_{ui} - s_{u1}}{L}\right)$$
$$\bar{\gamma}_{li} = \bar{\gamma}_{sl} \times \left(1 - \lambda \times \frac{s_{li} - s_{l1}}{L}\right) \quad \ldots (4)$$

where λ is the vorticity dispersion factor, S_{ui} and S_{li} are the distances along upper and lower wake from the separation points to the mid-points of the i-th wake panels, S_{u1} and S_{l1} are the lengths of the first upper and lower wake panels and L is the length of the cylinder.

The boundary condition of zero normal velocity at the collocation points of the N surface panels can be expressed as

$$\left(\frac{dy}{dx}\right)_j = \frac{\bar{v}_j + \mathrm{Sin}\alpha}{\bar{u}_j + \mathrm{Cos}\alpha} \quad \ldots (5)$$

where α is the angle of incidence. Satisfying the boundary condition at the midpoints of N surface panels gives N linear algebraic equations involving (N+2) unknown singularity strengths.

For the case of square and rectangular cylinders at zero angle of incidence, the separation points are fixed at the corner points of the front face. For this case, Kutta condition applied is that the sum of the vorticity strengths at the upper and lower separation points is zero, which ensures net zero vorticity shedding in the wake

$$\bar{\gamma}_{su} + \bar{\gamma}_{sl} = 0 \quad \ldots (6)$$

For the other three flow regimes at non zero angles of incidence, the point of confluence of the shear layers is not equidistant from the upper and lower separation points. The Kutta condition for such cases accounts for the unequal upper and lower shear layers and is given by zero vorticity at the wake closure

$$\gamma_c = \bar{\gamma}_{su} \times \left(1 - \lambda \times \frac{S_u - s_{u1}}{L}\right) + \bar{\gamma}_{sl} \times \left(1 - \lambda \times \frac{S_l - s_{l1}}{L}\right) = 0 \quad \ldots (7)$$

https://doi.org/10.1017/S0001924000001226 Published online by Cambridge University Press

where the subscript c stands for wake closure, S_u and S_l are the total lengths of the upper and lower shear layers, L is the length of the cylinder.

The other equation is obtained by satisfying the auxiliary condition at the trailing edge

$$\gamma_1 = \gamma_{N+1} \quad \ldots (8)$$

The (N+2) unknown strengths are solved simultaneously by the method of matrix inversion. Once the solution is obtained, the perturbation velocity components on the cylinder surface can be recalculated from Equations (1) and (2). The magnitude of total velocity can be obtained as

$$\bar{q}_j = \sqrt{\left(\bar{u}_j + \mathrm{Cos}\alpha\right)^2 + \left(\bar{v}_j + \mathrm{Sin}\alpha\right)^2} \quad \ldots (9)$$

The pressure coefficient at the collocation point of the j-th surface panel can be obtained as

$$C_{P_j} = 1 - \bar{q}_j{}^2 \quad \ldots (10)$$

3.0 THE ITERATIVE CALCULATION OF WAKE SHAPE

The shear layers emanating from the upper and lower separation points are initially assumed to be straight. The final wake shape is calculated iteratively.

Once the initial solution is obtained based on the assumed shape, velocities are recalculated at the midpoints of the panels on the shear layers. The new shape is then determined by piecewise integration starting from the separation points. At every iteration, the wake influence coefficients only need to be recalculated. Convergence of the solution is usually achieved within 10-15 iterations.

It may be noted that the length of a shear layer is dependent upon the vorticity dispersion factor (λ) only. For example, the length of the upper shear layer, S_u can be calculated from Equation (4), as follows

$$S_u = \frac{L}{\lambda} + s_{u1} \quad \ldots (11)$$

4.0 THE WAKE PRESSURE CALCULATION

Due to the viscous dissipation in the wake region of a real flow, there is a decrease in total pressure. The total pressure in the wake region is lower than that of the zone outside it. Application of Bernoulli's equation between a point in the free stream and a point inside the wake gives

$$p_\infty + \frac{1}{2}\times\rho\times U_\infty^2 = p_{inner} + \frac{1}{2}\times\rho\times q_{inner}^2 + \Delta H \quad \ldots (12)$$

where ΔH is the decrease in total pressure in the wake over that in the free stream. From the above equation the underpressure coefficient in the wake can be computed as

$$C_{P_{wake}} = \frac{p_{inner} - p_\infty}{\frac{1}{2}\times\rho\times U_\infty{}^2} = 1 - \left(\frac{q_{inner}}{U_\infty}\right)^2 - \frac{\Delta H}{\frac{1}{2}\times\rho\times U_\infty{}^2} \quad \ldots (13)$$

The jump in the total pressure across a free shear layer can be calculated by assuming zero static pressure drop across it. The average velocity in the upper shear layer is given by

$$q_{av}\big|_{upper} = \tfrac{1}{2}\times\left[q_{outer}\big|_{upper} + q_{inner}\big|_{upper}\right] \quad \ldots (14)$$

The vorticity in the upper shear layer is given as

$$\gamma_{ui} = q_{outer}\big|_{upper} - q_{inner}\big|_{upper} \quad \ldots (15)$$

$q_{outer}\big|_{upper}$ and $q_{inner}\big|_{upper}$ in terms of the shear layer vorticity can be obtained as follows

$$\begin{aligned} q_{outer}\big|_{upper} &= q_{av}\big|_{upper} + \tfrac{1}{2}\times\gamma_{ui} \\ q_{inner}\big|_{upper} &= q_{av}\big|_{upper} - \tfrac{1}{2}\times\gamma_{ui} \end{aligned} \quad \ldots (16)$$

The vorticity strength at the mid-point of the i-th upper wake panel is obtained from Equation (4). Jump in total pressure across upper shear layer can be computed as $\Delta H\big|_{upper} = [H_{outer} - H_{inner}]_{upper}$

$$= \tfrac{1}{2}\times\rho\times\left[q_{outer}\Big|_{upper}^2 - q_{inner}\Big|_{upper}^2\right] = \rho\times\gamma_{ui}\times q_{av}\big|_{upper} \quad \ldots (17)$$

Substitution of Equation (17) in Equation (13) gives

$$\left(C_{P_{wake}}\right)_{upper} = \left(\frac{p_{inner} - p_\infty}{\frac{1}{2}\times\rho\times U_\infty{}^2}\right)_{upper} = 1 - \left(\frac{q_{inner}}{U_\infty}\right)_{upper}^2 - \left(\frac{\rho\times\gamma_{ui}\times q_{av}}{\frac{1}{2}\times\rho\times U_\infty{}^2}\right)_{upper} \quad \ldots (18)$$

An expression for the coefficient of pressure in the wake region along the lower shear layer can be derived in a similar manner. The value of q_{av} is assumed to be equal to the velocity induced at the collocation point of the i-th wake panel.

5.0 COMPUTER CODE

A code has been developed in Fortran language to obtain pressure distribution on an arbitrary two-dimensional body geometry using a separation flow model based on panel technique. The source code is 31kb in size. The code takes around one minute to iteratively calculate the body surface pressure distribution and the converged wake shape. In the present investigation for solving separated flow past square and rectangular cylinders, four different versions of the code covering a range of angle of incidence from 0° to 45° have been developed. The numerical simulations were performed on a Pentium-III PC.

6.0 WIND TUNNEL TESTING

Wind tunnel tests were undertaken on a low speed wind tunnel at a Reynolds number of $1{\cdot}96 \times 10^5$. The wind tunnel is an open circuit suction type tunnel with test section size of 61cm × 61cm. The models tested in the wind tunnel were a square cylinder and a rectangular cylinder of aspect ratio of 2·0. The tests were carried out with a systematic variation of the angle of incidence of the bodies in steps of 5° from 0° to 45°. Pressures were measured on 44 ports on the surface of square cylinder and rectangular cylinder models by a single transducer using a Scanivalve system. The pressure plot obtained was integrated to obtain the lift and drag coefficients.

7.0 RESULTS AND DISCUSSION

Figure 2(a)-(d) show the comparison between Low Speed Wind Tunnel test results for Re = $1{\cdot}96 \times 10^5$ and results of numerical panel code for the surface pressure distribution on a square cylinder at various angles of incidence in the range $0 \le \alpha \le 45°$. Reasonable agreement is obtained between the experimental and numerical results for all cases for particular values of vorticity dispersion factor.

https://doi.org/10.1017/S0001924000001226 Published online by Cambridge University Press

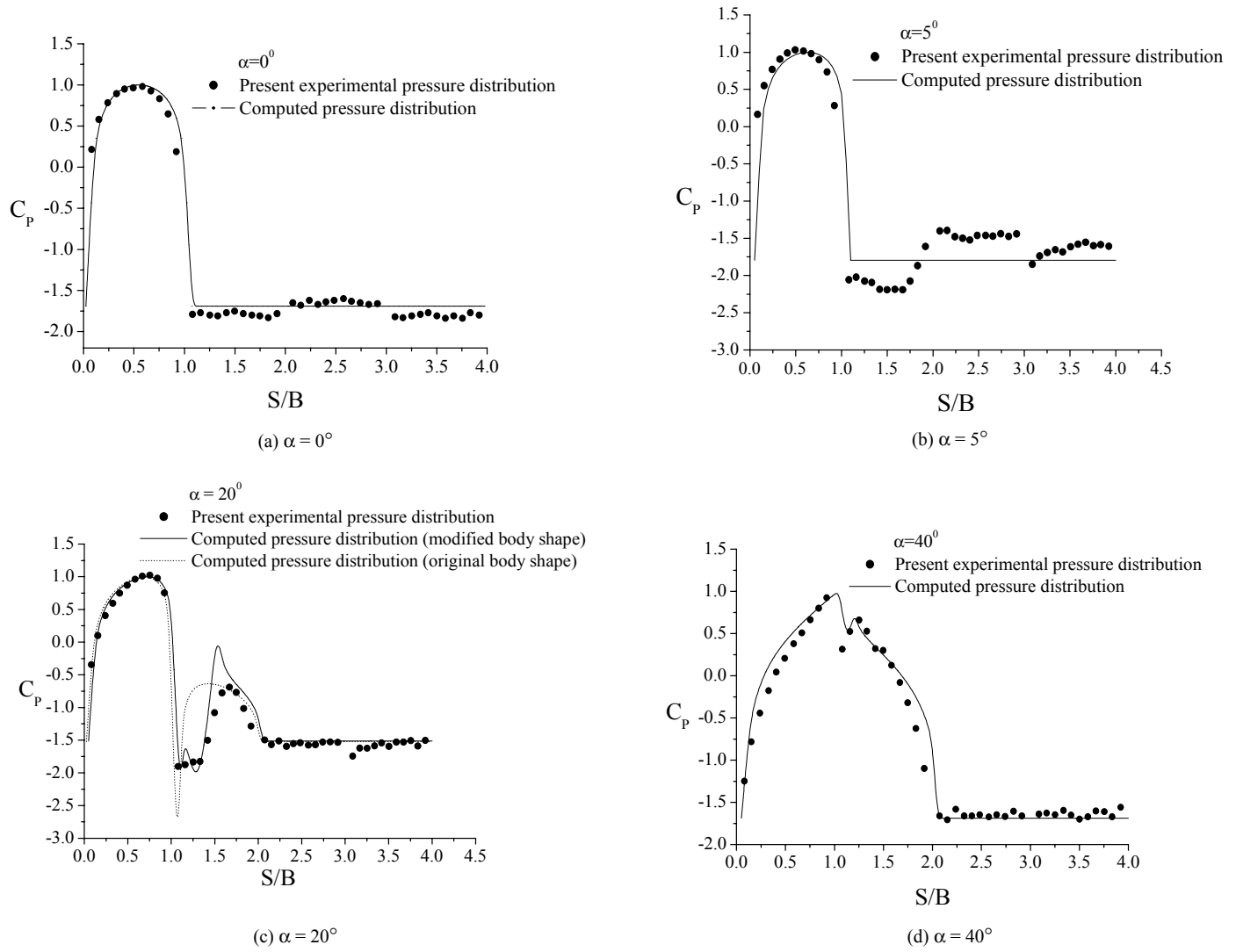


Figure 2. Comparison between low speed wind tunnel results and results of numerical panel code for square cylinder.

For $\alpha = 0°$, flow separates from the top and bottom corner of the front face of the cylinder and the computed pressure on top, rear and bottom surfaces is essentially constant in this separated region and compare well with experimental values (Fig. 2(a)).

For $\alpha = 5°$, the separated flow model for low angle of incidence has been applied and the computed results compare well with experimental results as shown in Fig. 2(b).

The location of the reattachment point on the lower face of square cylinder as a function of angle of incidence was obtained from Igarashi[5] and used as input to the numerical model for moderate angle of incidence. Body surface panels were distributed on the separation bubble surface and the pressure distribution on the bubble was assumed to be equal to the pressure acting on the body surface below the bubble. This method of "modified body shape" produced a pressure distribution on the bottom surface that was in close conformity with experimental results in the moderate angle of incidence regime. In Fig. 2(c), for $\alpha = 20°$, it is observed that the 'modified body approach' produces a pressure distribution which is in good agreement with the experimental pressure distribution. To illustrate the advantage of the 'modified body shape' results obtained with the original body shape (assuming attached flow throughout the bottom surface) is also plotted in the same figure. This result shows a large spurious dip in the computed pressure near the leading edge of the lower surface.

For angles of incidence higher than 35°, the separated flow model for the high angle of incidence has been applied and the computed results compare well with experimental results as shown for $\alpha = 40°$ in Fig. 2(d). Computed lift and drag, obtained by integration of body surface pressure distribution are shown in Fig. 3. The computed results compare reasonably well with the experimental results of Lee[1] and Igarashi[3].

The computed wake shape at $\alpha = 25°$ is shown in Fig. 4. It is observed that the upper and lower shear layers approach each other closely in the wake of the cylinder. The shear layers become almost parallel and are oriented in the direction of the free stream. The computed wake underpressure distribution for the upper and lower shear layers at $\alpha = 25°$ is shown in Fig. 5. The underpressure value approaches the free stream value asymptotically at the wake closure.

Aspect ratio, AR, of rectangular cylinder is defined as the length (L) to height (B) ratio of a rectangular cylinder, i.e., $AR = L/B$. Surface pressure distribution over a rectangular cylinder of $AR = 2{\cdot}0$ have been computed for various angles of incidence. Different models for various angles of incidence, as elaborated in the case of square cylinder, have been developed for the rectangular cylinder of $AR = 2{\cdot}0$ based on the data on reattachment angle presented by Da Matha Sant Anna *et al*[8]. For this case, reattachment angle is shown to be 7° by Da Matha Sant Anna *et al*[8]. Therefore for $0° < \alpha < 7°$,

https://doi.org/10.1017/S0001924000001226 Published online by Cambridge University Press

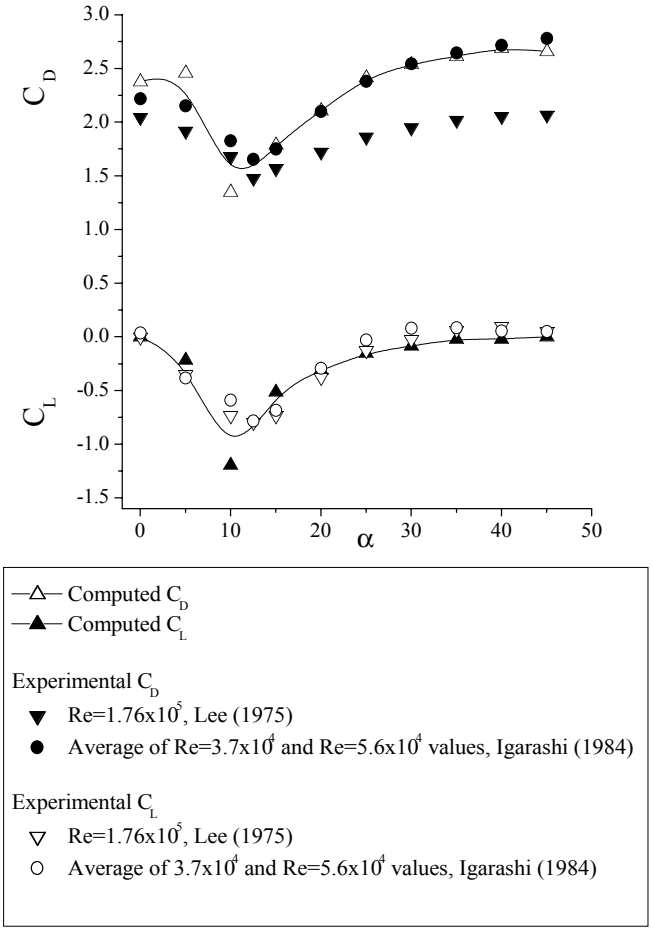


Figure 3. Comparison of computed C_D and C_L values with results of Lee[1] and Igarashi[3].

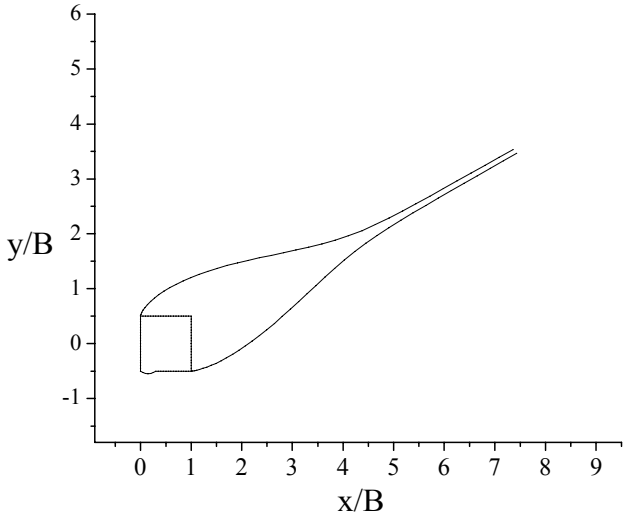


Figure 4. Computed wake shape for square cylinder; α = 25°, λ = 0·14.

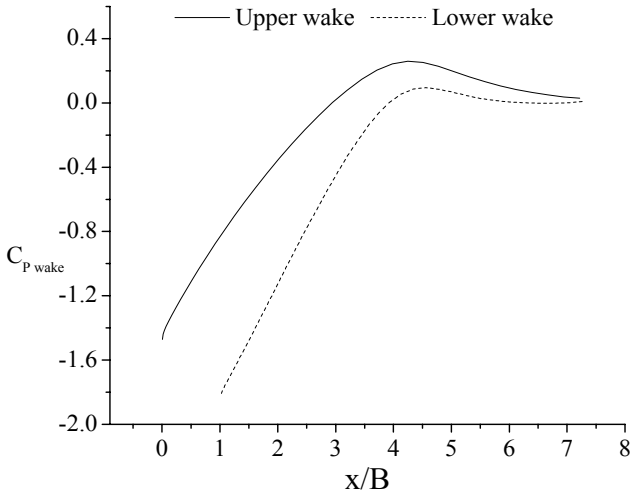
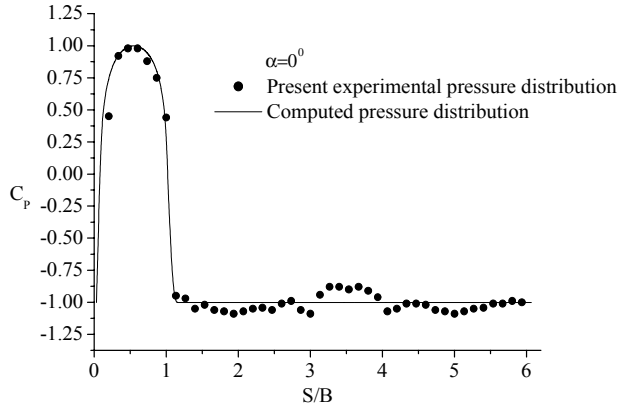
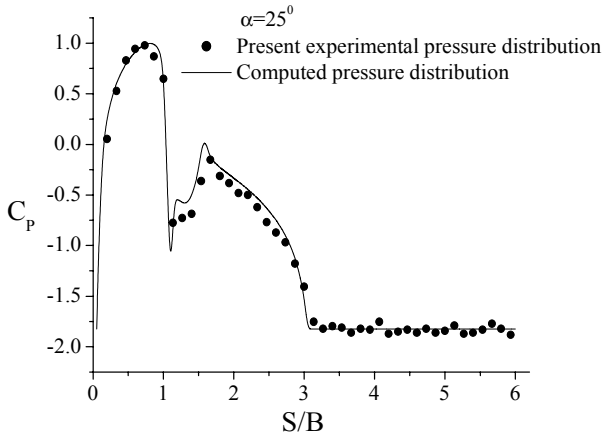


Figure 5. Computed wake underpressure for square cylinder; α = 25°, λ = 0·14.



(a) α = 0°



(b) α = 25°

Figure 6. Comparison between low speed wind tunnel results and results of numerical panel code for rectangular cylinder of AR = 2·0.

model of asymmetric wake with separation points on the front face is applied and for 7° < α < 30°, model with reattachment on the bottom face is applied.

For validation of the numerical calculation experimental work related to pressure measurement was undertaken on a rectangular cylinder of AR = 2.0 in the low speed wind tunnel at Re = 1·96 × 10^5 for various angles of incidence. Comparison between computed and experimental results, shown in Fig. 6(a) and (b) for α = 0° and 25°, is fairly good.

The panel code was applied to solve flow past rectangular cylinders of AR varying from 0·5 to 4·0 at α = 0°. For cylinders up to AR = 2·5 the flow was modelled without the separation bubble. For AR = 3·0 and AR = 4·0 a pair of separation bubbles were modelled on the top and bottom

https://doi.org/10.1017/S0001924000001226 Published online by Cambridge University Press

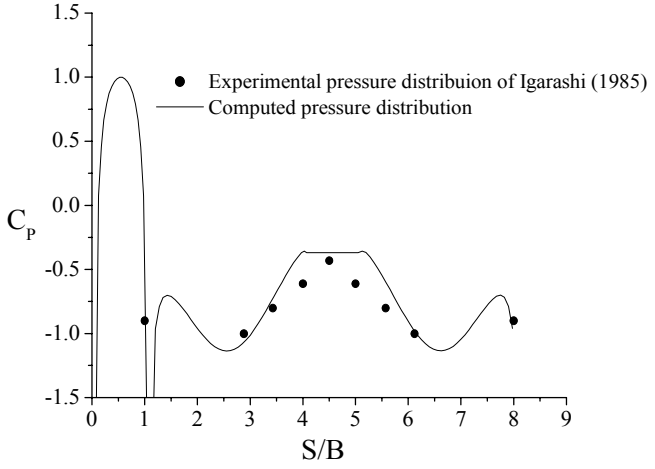


Figure 7. Comparison between experimental results and results of numerical panel code for rectangular cylinder of $AR = 3{\cdot}0$.

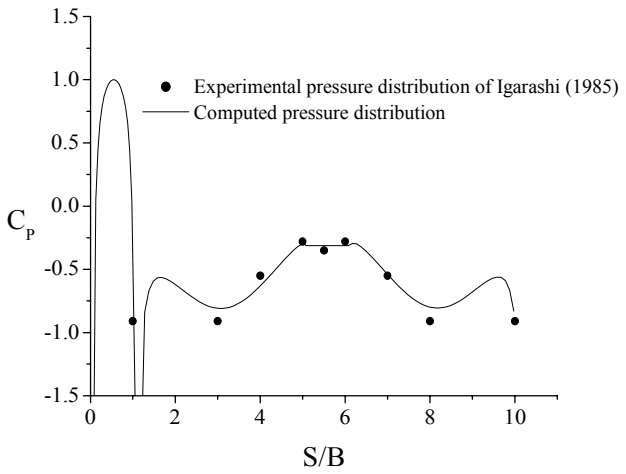


Figure 8. Comparison between experimental results and results of numerical panel code for rectangular cylinder of $AR = 4{\cdot}0$.

sides of the cylinder. For these higher aspect ratio cylinders the flow separates initially from the corners of the front face and subsequently reattaches at some point on the top and bottom faces before finally separating from the corners of the rear face. The pair of separation bubbles that form on the top and bottom faces are modelled by the 'modified body approach'. Fairly good agreement has been obtained between experimental (Igarashi[5]) and computed pressure distribution for $AR = 3.0$ and $4{\cdot}0$ as shown in Fig. 7 and Fig. 8 respectively.

8.0 CONCLUSIONS

- A line vortex model which combines a panel technique employing linearly varying vorticity and constant source singularity distribution on the body and constant vorticity 'free vortex lines' in the wake has been developed for calculation of separated flows around two-dimensional square and rectangular geometries.
- For solving separated flow past square and rectangular cylinders at angle of incidences ranging between 0º-45º, four different versions of the model have been developed to cater for zero, low, moderate and high angles of incidence.
- A 'modified body approach' has been formulated to model the separation bubble occurring on the bottom face of the cylinder at moderate angles of incidence. This technique was effective in obtaining good conformity with the experimental pressure distribution on the bottom face of the cylinder.
- Experimental investigations were carried out in a low speed wind tunnel to obtain the surface pressure distribution on a square and a rectangular cylinder of $AR = 2{\cdot}0$ at various angles of incidence varying between 0º-45º. This detailed surface pressure distribution has been used to compare the numerical results obtained by the potential flow model.
- Fairly good conformity has been obtained between the numerically computed and experimental pressure distribution on the surface of the square and rectangular cylinders for varying aspect ratios and angles of incidence.

REFERENCES

1. LEE, B.E. The effect of turbulence on the surface pressure field of a square prism, *J Fluid Mech*, 1975, **69**, (2), pp 263-282.
2. ROBERTSON, J.M., WEDDING, J.B., PETERKA, J.S. and CERMAC, J.E. Wall pressures of separation- reattachment flow on a square prism in uniform flow, *J Wind Engg Ind Aerodyn*, 1978, **2**, pp 345-359.
3. IGARASHI, T. Characteristics of the flow around a square prism, *Bulletin of JSME*, 1984, **27**, (231), pp 1858-1865.
4. CHEN, J.M. and LIU, C.H. Vortex shedding and surface pressures on a square cylinder at incidence to a uniform air stream, *Int J Heat and Fluid Flow*, 1999, **20**, pp 592-597.
5. IGARASHI, T. Characteristics of the flow around rectangular cylinders (the case of the angle of attack 0 deg.), *Bulletin of JSME*, 1985, **28**, (242), pp 1690-1696.
6. SAM, R.G., LESSMAN, R.C. and TEST, F.L. An experimental study of flow over a rectangular body, *J Fluids Engg*, 1979, **101**, pp 443-448.
7. BEARMAN, P.W. and TRUEMAN, D.M. An investigation of the flow around rectangular cylinders, *Aero Q*, 1972, **23**, (3), pp 229-237.
8. DA MATHA SANT ANNA, F.A., LANEVILLE, A., TREPANIER, J.Y. and LU, Z.Y. Detailed pressure field measurements for some 2-D rectangular cylinders, *J Wind Engg Ind Aerodyn*, 1988, **28**, pp 241-250.
9. LANEVILLE, A. and YONG, L.Z. Mean flow patterns around two-dimensional rectangular cylinders and their interpretation, *J Wind Engg Ind Aerodyn*, 1983, **14**, pp. 387-398.
10. OBASAJU, E. An investigation of the effects of incidence on the flow around a square section cylinder, *Aero Q*, 1983, **34**, pp 243-259.
11. NAKAGUCHI, H., HASHIMOTO, K. and MUTO, S. An experimental study on aerodynamic drag of rectangular cylinders, *J Japanese Soc Aero Space Science*, 1968, **16**, pp 1-5.
12. BOSTOK, B.R. and MAIR, W.A. Pressure distribution and forces on rectangular and D- shaped cylinders, *Aero Q*, 1972, **23**, pp 1-6.
13. SARPKAYA, T. Computational Methods with Vortices – The 1998 Freeman Scholar Lecture, *J Fluids Engg*, 1989, **111**, pp 5-52.
14. INAMURO, T., ADACHI, T. and SAKATA, H. A numerical analysis of unsteady separated flow by vortex shedding model, *Bulletin of JSME*, 1983, **26**, (222), pp 2106-2112.
15. SARPKAYA, T. and IHRIG, C.J. Impulsively-started flow about rectangular prisms- experiments and discrete vortex analysis, *J Fluids Engg*, 1986, **108**, pp 47-54.
16. NAGANO, S., NAITO, M. and TAKATA, H. A numerical analysis of two-dimensional flow past a rectangular prism by a discrete vortex model, *Computers and Fluids*, 1982, **10**, (4), pp 243-259.
17. STANSBY, P.K. A generalized discrete-vortex method for sharp-edged cylinders, *AIAA J*, 1985, **23**, (6), pp 856-861.
18. SARPKAYA, T. and SCHOAFF, R.L. Inviscid model of two-dimensional vortex shedding by a circular cylinder, *AIAA J*, 1979, **17**, (11), pp 1193-1200.
19. BASUKI, J. and GRAHAM, J.M.R. Discrete vortex computation of separated airfoil flow, *AIAA J*, 1987, **25**, (11), pp 1409-1410.
20. MASKEW, B. and DVORAK, F.A. The prediction of Clmax using a separated flow model, *J American Heli Soc*, 1978, **23**, pp 2-8.
21. RIBAUT, M. A vortex sheet method for calculating separated two-dimensional flows, *AIAA J*, 1983, **21**, (8), pp 1079-1084.
22. MUKHERJEA, S. and BANDYOPADHYAY, G. Separated flow about a wedge, *Aeronaut J*, 1990, **94**, (936), pp 196-202.

https://doi.org/10.1017/S0001924000001226 Published online by Cambridge University Press